Single-Molecule Imaging of Platinum Ligand Exchange Reaction Reveals Reactivity Distribution

N. Melody Esfandiari,[†] Yong Wang,[†] Jonathan Y. Bass, Trevor P. Cornell, Douglas A. L. Otte, Ming H. Cheng, John C. Hemminger, Theresa M. McIntire, Vladimir A. Mandelshtam, and Suzanne A. Blum*

Department of Chemistry, University of California, Irvine, California 92697

Received June 23, 2010; E-mail: blums@uci.edu

Abstract: Single-molecule fluorescence microscopy provided information about the real-time distribution of chemical reactivity on silicon oxide supports at the solution−surface interface, at a level of detail which would be unavailable from a traditional ensemble technique or from a technique that imaged the static physical properties of the surface. Chemical reactions on the surface were found to be uncorrelated; that is, the chemical reaction of one metal complex did not influence the location of a future chemical reaction of another metal complex.

The distribution of reactivity traditionally complicates the analysis of silicon oxide supported metal complexes,[1−3] which are used in numerous catalytic processes, including industrial processes.[1,4−6] Modification of the silicon oxide surface with a silyloxy reagent is a common strategy for tethering the metal complex to the surface.[4,5,7,8] Irregular surface features on glass and silica surfaces modified with silyloxy reagents have been studied by AFM;[9,10] however, a disconnect exists between this information regarding static surface physical features on the multimicrometer scale and the chemical reactivity of that surface in solution. Single-molecule fluorescence microscopy techniques are powerful methods to detect reactivity distributions in biophysical systems[11−22] but have not yet received widespread adaptation to chemical transformations.[23−29] Herein we demonstrate the ability of single-molecule fluorescence microscopy to bridge the information gap between imaging of the surface's static physical features and its dynamic chemical reactivity by revealing real-time information about the spatial distribution of chemical reactivity of a triethoxysilane-modified surface at the solution/surface interface. This level of detail would not be available by traditional analytical methods, including ensemble methods that average the collective properties of billions of molecules.

The general approach used in our experiments is shown schematically in eq 1. We examined the binding affinity of BODIPY-tagged (dien)platinum complex **1** (dien = diethylenetriamine) to glass microscope coverslips modified with *N,N′*-[3-(triethoxysilyl)propyl]thiourea.[9,10] We anticipated that the reaction of **1** with surface thiourea groups would rapidly immobilize the complex through platinum−sulfur covalent bond formation to form **2**, in analogy to the well-established ligand exchange chemistry of **1** in solution (eq 1).[30]

We used total internal reflection fluorescence (TIRF) microscopy[31,32] to image individual surface chemical reactions of **1** because only platinum complexes that were bound to the surface were detected, and molecules of **1** that remained in solution were not detected because they were not excited and/or because they were diffusing
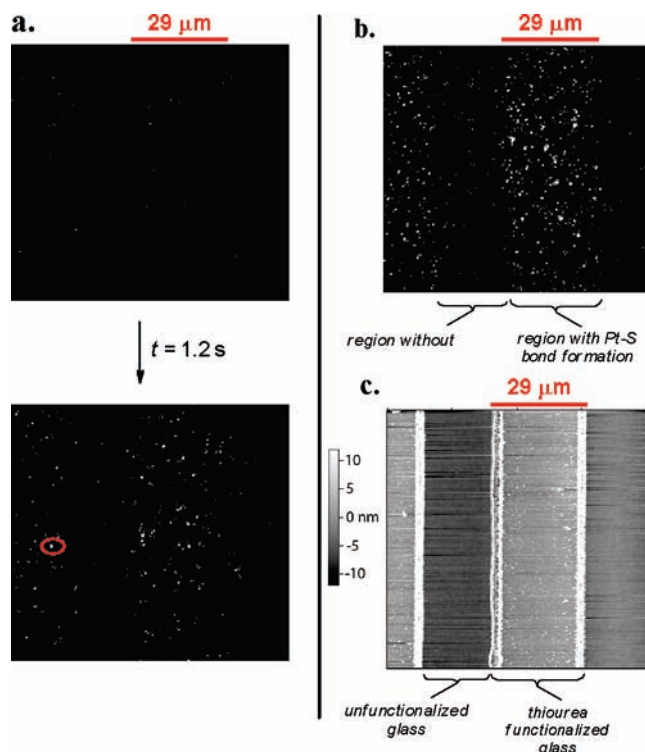

Figure 1. (a) Chemical reactions on patterned surface, 80×73 μm², showing heterogeneous distribution of reactivity after 1.2 s. Each white spot that appears indicates one Pt−S chemical reaction that occurred during the imaging; example individual platinum complex circled in red. (b) Composite image of 0−7.2 s. (c) AFM image of patterned surface, 80×80 μm² (thiourea, light gray; unfunctionalized glass, dark gray).

rapidly.[32] The individual platinum complexes on the surface displayed quantized binding and photobleaching events, which are established characterization fingerprints of single molecules (examples in Figures S5−S7).[33] Thus, the appearance of one fluorescence signal characterized the surface chemical reaction of one complex (Figure 1a).

We investigated the ability of the single-molecule technique to correlate surface physical inhomogeneity with chemical reactivity. A physically heterogeneous surface was created by patterning coverslips with alternating 25 μm stripes of thiourea and unfunctionalized glass, using a photopatterning process. The patterned coverslips were then employed as substrates for the chemical reaction with **1**. Stripes that contained the thiourea functional groups were found to recruit fluorophore-tagged platinum complexes significantly faster than stripes that were not functionalized (Figure 1a, 80×73 μm² field of view). In Figure 1a and b, each individual

---

[†] These authors contributed equally.

white spot is one covalently bound platinum complex that under-went a chemical reaction during the imaging.
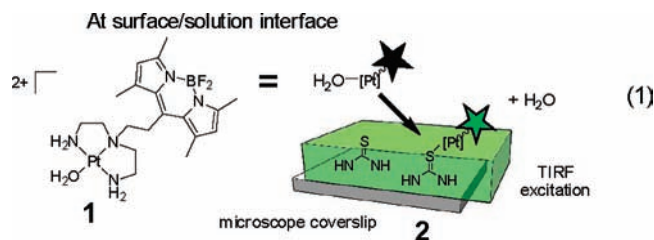
We were first concerned with the fact that we were imaging Pt−S covalent chemical reactivity and not surface physisorption.[34] A series of control experiments lacking any sulfur or platinum functionality confirmed the specificity of the surface chemical reaction. For example, physisorption of the BODIPY tag accounted for less than 2% of all binding events, as determined by comparing the binding of control compound **3** to the thiourea surface to a separate sample of **1** to the thiourea surface. The attachment of the platinum complex to the surface thiourea groups was confirmed to be covalent in nature via XPS characterization of the platinum−sulfur covalent bond on the surface (Figure 2). Specifically, two doublets provided the best fit for the XPS data of both **2** and **4**, and in both complexes these peak maxima were at 71.0 and 72.3 eV. The similarity by XPS between potential thiourea complex **2** and authentic thiourea complex **4** indicated that the binding of (dien)-platinum complexes to the thiourea surface was predominantly via covalent bond formation between the platinum and thiourea sulfur. The XPS experiments confirming covalent bond formation are further detailed in the Supporting Information.
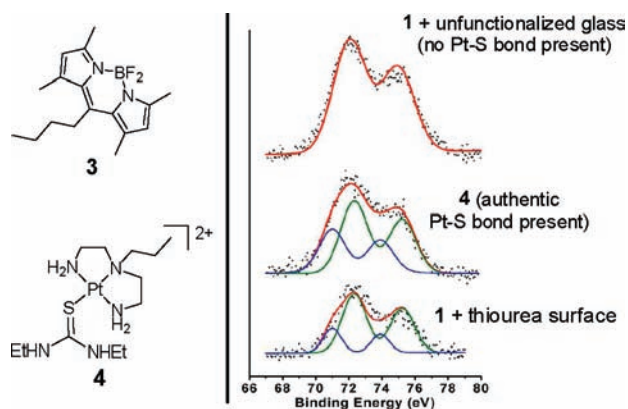

Figure 2. Comparison of XPS raw data and fitting Pt binding energies shows similarity between surface-bound Pt and authentic Pt-thiourea complex. Top: **1** on glass surface. Middle: **4**, authentic Pt−thiourea covalent bond. Bottom: Pt bound to thiourea-functionalized surface.

AFM imaging of the patterned surface showed the raised stripes of thiourea (Figure 1c; light gray) and lower stripes of unfunction-alized glass (dark gray). Additional 2 μm surface features were detected at the interface of the thiourea and unfunctionalized glass regions (white). These features likely corresponded to residual photoresist at the interface of the two regions.[35] Although these 2-μm regions showed different static physical features by AFM, they shared similar chemical reactivity properties to the thiourea surface, thereby supporting that these regions were thiourea-coated. Specifically, the reactive regions were 29 μm wide as measured by single-molecule fluorescence microscopy, which is the sum of the widths of the white and light gray surface features visible by AFM.

The spatial reactivity distribution across the patterned surface was quantified by measuring the distance between each individual chemical reaction; this measurement provided a level of detail that is not available through traditional ensemble experiments. Specifically, we estimated the radial pair correlation function $\rho(r)$, i.e., the probability distribution of finding two binding events separated from each other by distance r under the reaction conditions (Figure 3a, black). When compared to a probability distribution $\rho(r)$ for a generated set of random points uniformly distributed within the same domain (red curve), the experimental data display a significant decrease in the number of reactions that occurred at intermediate distances, consistent with the reactivity anticipated for a striped pattern.[36,37]
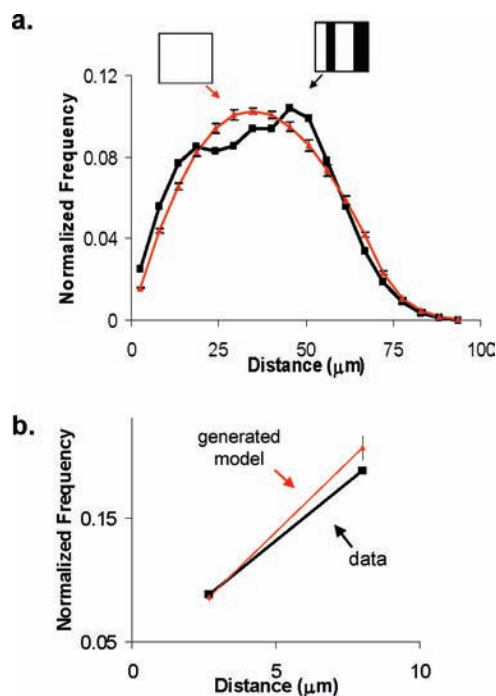

Figure 3. (a) Observed radial pair correlation function of **1** on striped surface, black, and generated uniform distribution with error bars, red. Difference shows degree of nonuniformity. (b) Observed radial pair correlation function of **1** within a subset of the thiourea surface, black, and generated uniform noncorrelated distribution, red, with error bars. Similarity at short distances established that binding events are noncorrelated.

The ability to localize individual events also permitted the probing of whether or not the chemical reaction of one platinum complex influenced the location of a future chemical reaction (e.g., if the chemical reactions were correlated). In order to probe this correlation, the reactions within a 32 μm^2 subset of a thiourea stripe were analyzed. At short distances, where correlation would be most likely, our data closely match a generated set of noncorrelated data (Figure 3b).[38,39] This similarity established that chemical reactions on the thiourea surface were noncorrelated; i.e., the chemical reaction of one platinum complex did not influence the location of a future chemical event.

In conclusion, the ability to localize single chemical events by fluorescence microscopy bridges the information gap between the static physical properties of the silyloxy-functionalized surfaces detectable by AFM and the distribution of real-time chemical reactivity at the solution−surface interface on the multimicrometer scale. The measurement of the distances between each individual chemical reaction provided a level of detail of the reactivity distribution that is unavailable through an ensemble technique.

Given that heterogeneous catalysts on functionalized oxide supports are used in many industrial processes and that determining the spatial distribution of reactivity is a key challenge in these systems,[1] a broad potential application area exists for this single-molecule technique. A full report expanding on this single-molecule strategy is forthcoming.

Supporting Information Available: Experimental procedures and compound characterization. This material is available free of charge via the Internet at http://pubs.acs.org.

References

(1) Wekhuysen, B. M. *Angew. Chem., Int. Ed.* **2009**, *48*, 4910–4943.
(2) Bouchard, L. S.; Kovtunov, K. V.; Burt, S. R.; Anwar, M. S.; Koptyug, I. V.; Sagedeev, R. Z.; Pines, A. *Angew. Chem., Int. Ed.* **2007**, *46*, 4064–4068.
(3) Bouchard, L. S.; Burt, S. R.; Anwar, M. S.; Kovtunov, K. V.; Koptuyg, I. V.; Pines, A. *Science* **2008**, *319*, 442–445.
(4) Yin, L.; Liebscher, J. *Chem. Rev.* **2007**, *107*, 133–173.
(5) Heitbaum, M.; Glorius, F.; Escher, I. *Angew. Chem., Int. Ed.* **2006**, *45*, 4732–4767.
(6) Fink, G.; Steinmetz, B.; Zechlin, J.; Przybyla, C.; Tesche, B. *Chem. Rev.* **2000**, *100*, 1377–1390.
(7) Blümel, J. *Coord. Chem. Rev.* **2008**, *252*, 2410–2423.
(8) Yang, Y.; Beel, B.; Blümel, J. *J. Am. Chem. Soc.* **2008**, *130*, 3771–3773.
(9) Howarter, J. A.; Youngblood, J. P. *Langmuir* **2006**, *22*, 11142–11147.
(10) Wang, W.; Vaughn, M. W. *Scanning* **2008**, *30*, 65–77.
(11) Yildiz, A.; Tomishige, M.; Vale, R. D.; Selvin, P. R. *Science* **2004**, *303*, 676–678.
(12) van Oijen, A. M.; Blainey, P. C.; Crampton, D. J.; Richardson, C. C.; Ellenberger, T.; Xie, X. S. *Science* **2003**, *301*, 1235–1238.
(13) Lee, J.-B.; Hite, R. K.; Hamdan, S. M.; Xie, X. S.; Richardson, C. C.; van Oijen, A. M. *Nature* **2006**, *439*, 621–624.
(14) Ditzler, M. A.; Alemán, E. A.; Rueda, D.; Walter, N. G. *Biopolymers* **2007**, *87*, 302–316.
(15) Ha, T.; Ting, A. Y.; Liang, J.; Caldwell, W. B.; Deniz, A. A.; Chemla, D. S.; Schultz, P. G.; Weiss, S. *Proc. Natl. Acad. Sci. U.S.A.* **1999**, *96*, 893–898.
(16) Sako, Y.; Minoguchi, S.; Yanagida, T. *Nat. Cell Biol.* **2000**, *2*, 168–172.
(17) Kiel, A.; Kovacs, J.; Mokhir, A.; Krämer, R.; Herten, D.-P. *Angew. Chem., Int. Ed.* **2007**, *46*, 3363–3366.
(18) Bates, M.; Huang, Bo.; Dempsey, G. T.; Zhuang, X. *Science* **2007**, *317*, 1749–1753.
(19) Ritchie, K.; Iino, R.; Fujiwara, T.; Murase, K.; Kusumi, A. *Mol. Membr. Biol.* **2003**, *20*, 13–18.
(20) Greenleaf, W.; J.; Woodside, M. T.; Block, S. M. *Annu. Rev. Biophys. Biomol. Struct.* **2007**, *36*, 171–190.
(21) Roeffaers, M. B. J.; De Cremer, G.; Uji-i, H.; Muls, B.; Sels, B. F.; Jacobs, P. A.; De Schryver, F. C.; De Vos, D. E.; Hofkens, J. *Proc. Natl. Acad. Sci. U.S.A.* **2007**, *104*, 12603–12609.
(22) Martínez Martínez, V.; De Cremer, G.; Roeffaers, M. B. J.; Sliwa, M.; Baruah, M.; De Vos, D. E.; Hofkens, J.; Sels, B. F *J. Am. Chem. Soc.* **2008**, *130*, 13192–13193.
(23) Roeffaers, M. B. J.; Sels, B. F.; Uji-i, H.; De Schryver, F. C.; Jacobs, P. A.; De Vos, D.; Hofkens, J. *Nature* **2006**, *439*, 572–575.
(24) Xu, W.; Kong, J. S.; Chen, P. *Phys. Chem. Chem. Phys.* **2009**, *11*, 2767–2778.
(25) Ameloot, R.; Roeffaers, M.; Baruah, M.; De Cremer, G.; Sels, B. F.; De Vos, D.; Hofkens, J. *Photochem. Photobiol. Sci.* **2009**, *8*, 453–456.
(26) Shen, H.; Xu, W.; Chen, P. *Phys. Chem. Chem. Phys.* **2010**, *12*, 6555–6563.
(27) Roeffaers, M. B. J.; De Cremer, G.; Libeert, J.; Ameloot, R.; Dedecker, P.; Bons, A. J.; Bückins, M.; Martens, J. A.; Sels, B. F.; De Vos, D. E.; Hofkens, J. *Angew. Chem., Int. Ed.* **2009**, *48*, 9285–9289.
(28) De Cremer, G.; Roeffaers, M. B. J.; Bartholomeeusen, E.; Lin, K.; Dedecker, P.; Pescarmona, P. P.; Jacobs, P. A.; De Vos, D. E.; Hofkens, J. *Angew. Chem., Int. Ed.* **2010**, *49*, 908–911.
(29) Naito, K.; Tachikawa, T.; Fujitsuka, M.; Majima, T. *J. Phys. Chem. C* **2008**, *112*, 1048–1059.
(30) Gray, H. B. *J. Am. Chem. Soc.* **1962**, *84*, 1548–1552.
(31) Sako, Y.; Uyemura, T. *Cell Struct. Funct.* **2002**, *27*, 357–365.
(32) Axelrod, D. *Methods Enzymol.* **2003**, *361*, 1–133.
(33) Weiss, S. *Science* **1999**, *283*, 1676–1683.
(34) Wirth, M. J.; Legg, M. A. *Annu. Rev. Phys. Chem.* **2007**, *58*, 489–510.
(35) These features have been previously reported when employing SU-8 photoresist with trialkoxysilane reagents; see: Joshi, M.; Pinto, R.; Rao, V. R.; Mukherji, S. *Appl. Surf. Sci.* **2007**, *253*, 3127–3132.
(36) As can be observed in Figure 3a, the stripped pattern retains molecules at intermediate distances due to the lengthwise population of molecules within the stripe.
(37) The error bars for the calculated uniform distribution correspond to 1 standard deviation as derived from 10 000 simulations of uniform distribution.
(38) The initial points in Figure 3b differ from the initial points in Figure 3a because only a subset of the image was analyzed in Figure 3b.
(39) The potential for using high-resolution analysis exists; see: (a) Fernández-Suárez, M.; Ting, A. Y. *Nat. Rev. Mol. Cell Biol.* **2008**, *9*, 929–943. (b) Hell, S. W. *Science* **2007**, *316*, 1153–1158. (c) Reference 28.

JA105517D